Simulation Study on the Effect of PD Pulse Shape on Electromagnetic Wave Propagation in an L-type GIS Structure

Tao Zhao
Hebei Provincial Key Laboratory of Power Transmission Equipment Security Defense
North China Electric Power University
Baoding, China
T.Zhao@ncepu.edu.cn

Martin D. Judd
High Frequency Diagnostics and Engineering Ltd
Glasgow, UK
m.judd@hfde.co.uk

Brian G. Stewart
Institute of Energy and Environment
University of Strathclyde
Glasgow, UK
brian.stewart.100@strath.ac.uk

***Abstract*—Modeling of electromagnetic wave propagation inside a GIS structure can be beneficial to understanding and improvement in sensitivity of PD detection by providing information to help determine more optimal positions for UHF PD sensors. PD pulse shape is found to have a strong influence on the distribution of UHF electric field detected at sensors installed on the GIS. This paper focuses on the effect of different PD pulse shapes to understand better EM wave propagation behavior. The time dependent EM wave propagation behavior is simulated for 3 kinds of pulse shape with different front time, time to half-value and half amplitude width and a comparison is made based on the attenuation characteristic analysis of UHF sensor locations along an L-type GIS tank. The resulting influence of different PD pulse shape sources on the UHF sensor signals is presented and discussed. The results in this paper are conducive to understanding the limitations and optimization of PD sensor positions for UHF signal detection and PD location estimation.**

Keywords—electromagnetic wave, PD pulse shape, propagation behavior, UHF signal

I. Introduction

The UHF method has been widely used in PD detection and localization in GIS systems. Modeling of electromagnetic (EM) wave propagation inside a GIS structure can be helpful for understanding and improving the sensitivity of PD detection by providing information to help determine more optimal positioning of UHF PD sensors [1-2]. Propagation characteristics of radiated PD EM waves in GIS systems are complicated. When an EM wave spreads in a GIS system, several phenomena may occur (such as reflection, refraction, resonance, wave mode conversion and attenuation), which combine to cause complex EM wave behavior [3-4]. The propagated electric field distribution reveals that electric field differs for different positions after the EM wave signal passes through a GIS pipe. Therefore, for the electric field detection, the outputs of the sensors may have significant differences for different installation locations.

Obviously, many factors can affect the electric field distribution, such as the geometry and structure of a GIS system. A time-domain Gaussian current pulse with very narrow pulse width is most commonly used to represent a PD source in electromagnetic simulation methods. In addition the PD pulse width and shape are found to have a strong influence on the distribution of UHF electric field detected at sensors installed on the GIS.

This paper focuses on the effect of a PD pulse with different width and shape on the EM wave propagation behavior. Firstly, the time-dependent EM wave propagation behavior is simulated for 3 kinds of pulse shape with different front time (the time from zero to the peak), time to half-value and half amplitude width using COMSOL Multiphysics where a comparison based on different pulse shapes for the EM wave propagation behavior is conducted. Then, based on the attenuation characteristic analysis of UHF sensor locations along the L-type GIS tank and around its circumference, the resulting influence of different Gaussian pulse width sources on the UHF sensor signals is presented and discussed. The results in this paper are beneficial to understanding the limitations and optimization of PD sensor positions for UHF signal detection and localization.

II. Simulation Model

A. Model of L-type GIS Structure

The geometry of the L-type GIS structure used in this study is shown schematically in Fig. 1. The inner and outer diameters of the conductor and tank are 125 mm and 420 mm respectively. The conductors are represented as perfect electric conductors (PEC) in the COMSOL model. Sulfur hexafluoride (SF_6) is the insulation gas considered (relative permittivity ε_r = 1, relative permeability μ_r = 1, electrical conductivity σ = 0). Dielectric spacers are considered as epoxy resin (relative permittivity ε_r = 4, relative permeability μ_r = 1, electrical conductivity σ = 0). The field formulation used for the time-domain simulations is described by the following equations [5-6]:

$$\nabla\times\left(\frac{1}{\mu_r}\nabla\times\mathbf{A}\right)+\mu_0\sigma\frac{\partial\mathbf{A}}{\partial t}+\mu_0\frac{\partial}{\partial t}\left(\varepsilon_0\varepsilon_r\frac{\partial\mathbf{A}}{\partial t}\right)=0 \quad (1)$$

$$\mathbf{n}\times\mathbf{E}=0 \text{ (PEC boundary condition)} \quad (2)$$

$$Z_{port} = \frac{U_{port}}{I_{port}} \quad \text{(Lumped port with voltage input)} \qquad (3)$$

$$\mathbf{A}(\mathbf{r}, 0) = 0 \quad \text{(Zero initial condition)} \qquad (4)$$

where **A** is the magnetic vector potential, μ_0 represents the magnetic permeability of vacuum, μ_r is the relative magnetic permeability, ε_0 is the electric permittivity of vacuum, ε_r refers to the relative permittivity of the propagation medium, **n** is a unit vector normal to the surface and Z_{port} is the wave impedance of the lumped (input) port. The output port is set to a scatter boundary for modeling an open boundary and this boundary is transparent for incoming plane waves with any angle of incidence. Therefore there is no reflection back into the structure at the output port during the simulation.

Four point probe positions (A, B, C and D) and their coordinates are shown as red points in Fig. 1.

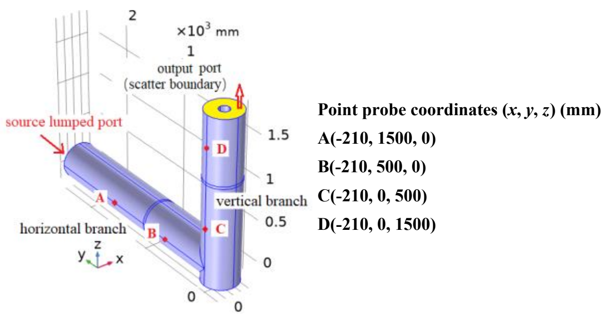

Fig. 1. L-type structure with two spacers and the locations of the point probes.

B. *Pulse shape of the PD source*

A time-domain Gaussian current pulse with very narrow pulse width is most frequently used to represent a PD source in electromagnetic simulation methods. As mentioned above, the PD pulse width and shape is found to strongly influence the distribution of electric field detected at UHF sensors installed on a GIS system.

To present the effect of PD pulse with different width and shape for the EM wave propagation behavior, the pulses shown in Fig. 2 are used in the simulation. There are 3 kinds of waveform with different front time, time to half-value and the half amplitude width, which are shown in Table I specifically. Time dependent plots of the electric field in the radial direction during a propagation time range are produced once the simulation is complete. Because of the differences of the duration for the three pulses, the time steps and ranges of the simulation also differ for the different pulses which are listed in Table I.

TABLE I. PULSE SHAPES AND THE SIMULATION TIME IN THE MODEL

Pulse number	Front time (ns)	Time to half-value (ns)	Half amplitude width (ns)	Time step (ns)	Simulation time (ns)
Pulse I	0.07	0.19	0.18	0.025	20
Pulse II	0.19	0.51	0.46	0.05	20
Pulse III	0.37	1.14	1.05	0.05	40

The pulses with different shapes were applied to the coaxial structure of the GIS at the input plane of the GIS busbar respectively. Because of the stochastic nature of PD, pulse amplitude is usually quite variable in practice. Hence, for the purpose of simulation, the model uses a normalized PD pulse amplitude and normalized electric field results are presented.

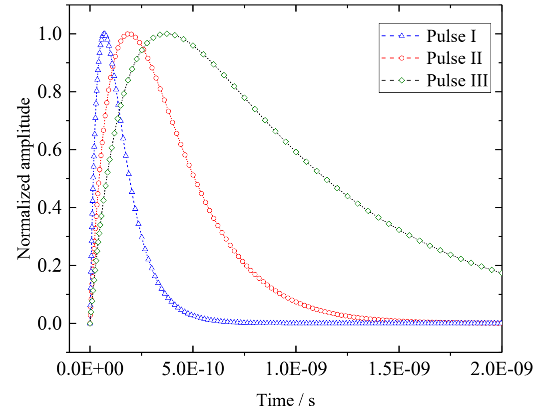

Fig. 2. Pulse shapes used in the simulation

III. SIMULATION RESULTS

A. *Attenuation Effect of Spacer and L bend*

The curves in Fig. 3 show the time-varying electric field at the point probes on the horizontal and vertical branches of the L-type structure. The electric field starts at zero and increases when the EM wave passes each point probe followed by a peak in the field curves. After that, the field curves start to fluctuate over time and there are many peaks with lower amplitudes generated by the reflection effect from the spacers and the L-bend. From the reflected waves in the plot, it can be seen that the spacer and the bend reflect part of the wave energy.

The EM waves become undulating as they propagate forward and the field distribution shows a significant difference after EM wave passes through the L-bend. The change of waveform and amplitude indicates an overlap of adjacent waves caused by the wave reflection. It can be observed that the electric field properties differ quite significantly for different positions when the EM wave propagates into the vertical branch.

Table II shows the attenuation of the EM wave passing by the spacer and L-bend. Because of the severe waveform distortion, in the attenuation calculation, the maximum value of the waveform amplitude within the simulation time is selected at point probe C and D. The result suggests that there are obvious differences in the attenuation characteristics for the three pulse waveforms. The attenuation effect of the spacer is represented by the difference between probe A and B. In this modeling, after passing through one spacer, the amplitude of the electric field reduces by about 23%, 8% and 5% at which probe points specifically. The electric field difference between probe C and D also represents the influence of the spacer but the results may be less valid because of the severe distortion and attenuation of the waveforms.

The attenuation effect of the L-bend is represented by the percentage change between probe B and C - they also differ for each of the three pulse shapes. Percentage amplitude changes are

51%, 45% and 23% respectively, which becomes smaller with the increase of the pulse duration. Pulse I has the shortest front time, half-value time and the half amplitude width and the most severe attenuation compared with the other two pulses.It can therefore be seen that the high frequency components of the EM wave are more affected by the attenuation of the bend.

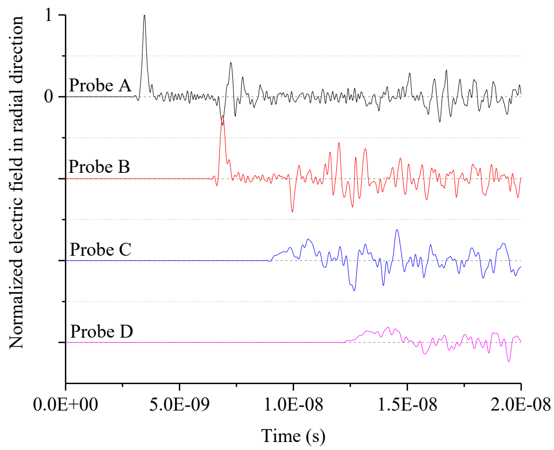

(a) Pulse I

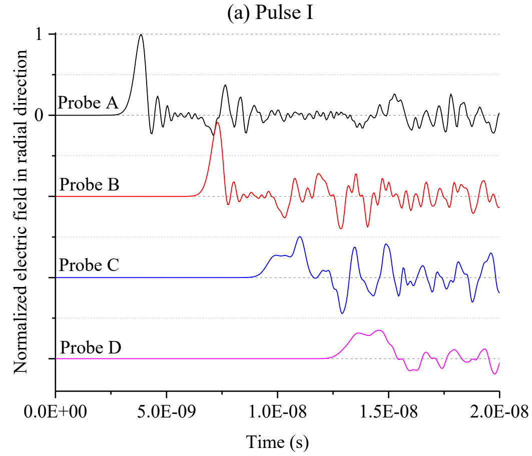

(b) Pulse II

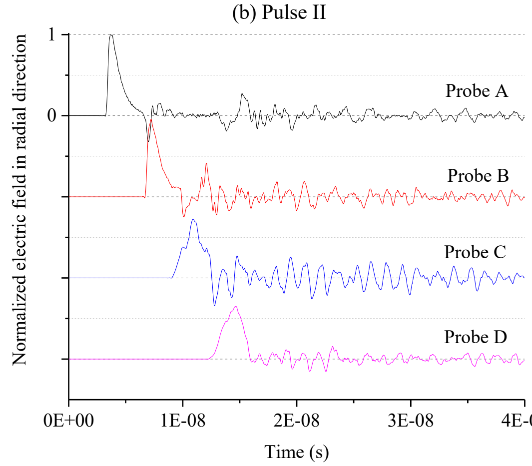

(c) Pulse III

Fig. 3. Electric field in radial direction versus time (the maximum on probe A is as the normalized benchmark for the three pulse shapes).

A similar result of attenuation effect was also presented in reference [7] which investigated the effects of the L-type GIS structure on the propagation characteristics of the EM wave propagating. It suggested that the L-type branch does not affect the TEM component of the EM wave, and that reflections are generated by higher frequency components above the TE11 mode. This consideration allows a prediction that the amplitude of the propagating EM wave will change significantly around an L-shaped branch when a PD source is located in the vicinity of the L-branch part because the TE mode is more likely to be overlapped with the TEM mode.

TABLE II. ATTENUATION OF EM WAVE FOR THE THREE PULSE SHAPES

Pulse shape	Normalized electric field in radial direction				
	Probe A	***Probe B***	***Probe C***	***Probe D***	***Percentage change between B and C***
Pulse I	100%	77%	38%	19%	51%
Pulse II	100%	92%	51%	35%	45%
Pulse III	100%	95%	73%	65%	23%

B. Effect on installation position of UHF sensor

The comparisons above indicates that the electric field properties differ significantly for different positions in the structure. Thus, for electric field detection, the outputs of UHF PD sensors may be very different for different installation positions. The difference of the electric field for different positions near the L-bend are compared below. The coordinates of 5 measurement positions are given in Fig. 4 - these locations are commonly used for PD UHF sensor installations. P1 and P2 are positioned before the L-bend, while P3, P4 and P5 are positioned in the same horizontal plane after the L-bend.

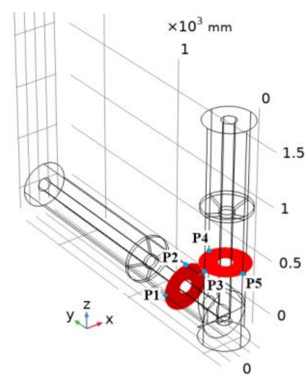

Fig.4. Point probe positions used for sensor installations in the model

The curves of the electric field in the radial direction at the 5 point probes are displayed in Fig. 5. It should be noted that for Pulse III, the largest waveform amplitude occurs at probe P4, so the normalized benchmark is the maximum of probe P4.

The electric field properties at probe P1 and P2 before the L-bend are very similar and there are only minor differences in the shape. In contrast, the electric field properties are very different at probes P3, P4 and P5 after the L-bend. Similarly, the maximum values of the waveform amplitude within the simulation time are selected and the attenuation for the three pulse shapes at point probes P3, P4 and P5 are shown in Table III. Significant differences in the attenuation characteristics can be seen at the three point probes.

It is indicated by comparison, that the attenuation at probe P3 is most severe and the detection sensitivity is higher at the other two probes i.e. P4 and P5. Therefore, the detection sensitivity at the probes in the horizontal direction (0°) of the L-bend is higher than that in the vertical direction (90°) if the drawing direction of the tank is defined to be the horizontal direction (0°). This result is consistent with that of reference [8]. Thus, if the location of the sensor is chosen appropriately, i.e. P4, the effect of the attenuation by the L-type structure can be minimized.

The effect of pulse shape at the probe positions is also displayed in Fig.4 and Table III. The attenuation is more severe for the pulse with the narrowest pulse width. This characteristic is also consistent with the result in Table II.

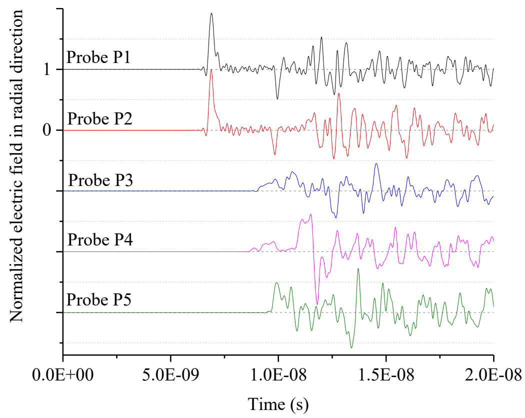

(a) Pulse I (the maximum on probe P2 is as the normalized benchmark)

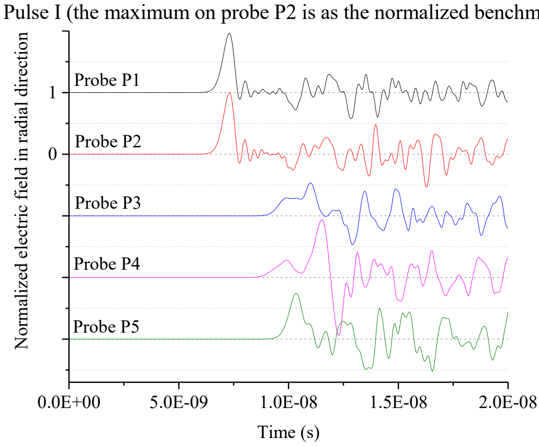

(b) Pulse II (the maximum on probe P2 is as the normalized benchmark)

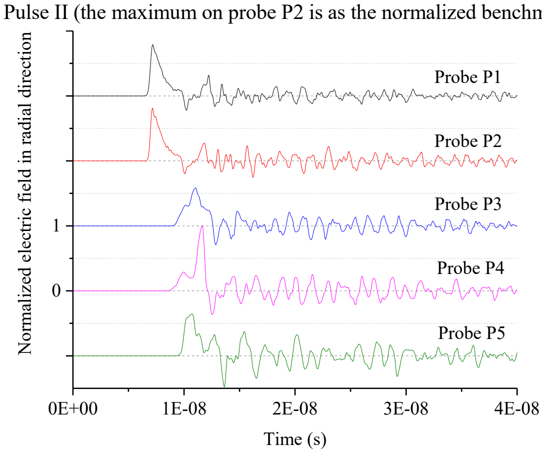

(c) Pulse III (the maximum on probe P4 is as the normalized benchmark)

Fig. 4. Comparison of electric field at point probes

TABLE III. ATTENUATION OF EM WAVE FOR THE THREE PULSE SHAPES PASSING BY L-BEND

Pulse shape	**Normalized electric field in radial direction**				
	P1	***P2***	***P3***	***P4***	***P5***
Pulse I	94%	100%	45%	87%	73%
Pulse II	96%	100%	53%	94%	74%
Pulse III	79%	81%	59%	100%	64%

IV. CONCLUSIONS

In this study, the effects of PD pulse shape on the EM wave propagation behavior has been investigated. Changes of waveform and amplitude are observed in an L-type GIS tank during the process of EM wave propagation.

It is indicated by comparison that there are obvious differences in the attenuation characteristics for the three pulse waveforms. In this modeling, after passing through one spacer, the amplitude of the electric field declines by about 23%, 8% and 5% respectively. The attenuation effect of L-bend are 51%, 45% and 23% represented by the percentage change respectively, which becomes smaller with increase of the pulse duration.

The detection sensitivity at the test point in the horizontal direction (0°) of the L-bend is higher than that in the vertical direction (90°). Therefore, if the location of the electric field detected by the sensor is chosen reasonably, the measurement sensitivity obtained can minimize the effects of attenuation introduced by the L-type structure. In addition, lower amplitude and field pulse increase as EM wave propagation may mean increased error in determining the time of arrival. Thus a compromise may be necessary between accurate detection and sensitivity.

REFERENCES

[1] J. S. Pearson, O. Farish, B. F. Hampton, M. D. Judd, D. Templeton, B. M. Pryor and I. M. Welch, “Partial discharge diagnostics for gas insulated substations,” IEEE Trans. Dielectr. Electr. Insul., vol. 2, no. 5, pp. 893-905, Oct. 1995.

[2] G. Behrmann, W. Koltunowicz and U. Schichler, “State of the Art in GIS PD Diagnostics,” 2018 Condition Monitoring and Diagnosis (CMD), Perth, WA, 2018, pp. 1-6.

[3] CIGRE WG D1.33, Tech. Brochure 502, “High-Voltage On Site Testing with Partial Discharge Measurement,” 2012.

[4] CIGRE WG D1.25, UHF partial discharge detection system for GIS: Application guide for sensitivity verification, CIGRE Tech. Brochure 654, 2016.

[5] G. Behrmann, K. Wyss, J. Weiss, et al, “Signal delay effects of solid dielectrics on time-of-flight measurements in GIS,” IEEE Trans. Dielectr. Electr. Insul., vol. 23, no. 3, pp. 1275-1284, 2016.

[6] J. Smajic, W. Holaus, J. Kostovic, et al, “3D Full-Maxwell Simulations of Very Fast Transients in GIS,” IEEE Trans. on Magnetics, vol. 47, no. 5, pp. 1514-1517, May 2011.

[7] M. Hikita, S. Ohtsuka, J. Wada, et al, “Propagation properties of PD-induced electromagnetic wave in 66 kV GIS model tank with L branch structure,” IEEE Trans. Dielectr. Electr. Insul., vol. 18, no. 5, pp. 1678-1685, Oct. 2011.

[8] T. Zhao, M. D. Judd and B. G. Stewart, “The time dependent simulation of PD electromagnetic wave propagation in GIS systems,” IEEE Conf. Electr. Insul. Dielect. Phenom (CEIDP), 2020, pp. 1-4.(in press)